Dynamic Distance Modulation and Active Site Separation in Ru_1-Ru_3@MoS_2 Catalyst for C-O Bond Activation

Shouqin Mu, Jiehang Wei, Tao Ma, Yuxin Xu, Wenjuan Wang, Mengjia Fu, Yingtao Liu, Xin Wang*,

School of Chemistry and Chemical Engineering, Ningxia University, Yinchuan 750021, China.

E-*mail address:* wangxin@nxu.edu.cn (X., Wang)

The binding energy of TM@MoS_2 (E_b) can be calculated as follows:

$$E_b = (E_{cat} - E_{2S-vacMoS_2} - E_{Ru(SA)} - E_{Ru(NC)})/n \quad (1)$$

Where E_{cat} represents the total energy of the catalyst, $E_{2S\text{-}vac\ MoS_2}$ denotes the energy of molybdenum disulfide containing two sulfur vacancies. $E_{Ru\ (SA)}$ denotes the energy of a metallic Ru_1 atom. $E_{Ru\ (NC)}$ represents the energy of the Ru_3 cluster. Where n represents the number of Ru atoms

$$\Delta G = \Delta E + \Delta E_{ZPE} - T\Delta S \quad (2)$$

The Gibbs free energy difference (ΔG) for each elementary reaction step is calculated according to Eq. S2, where ΔE, ΔE_{ZPE}, and ΔS represent the computed reaction (electronic) energy, zero-point energy difference, and entropy difference between the products and reactants at room temperature (T = 298.15 K), respectively.

The activation energy barrier (ΔG_{act}) for the initial reaction is calculated as follows:

$$\Delta G_{act} = G_{TS} - G_{IS} \quad (3)$$

G_{TS} and G_{IS} represent the transition state free energy and the initial state free energy, respectively.

The reaction free energy (ΔG_{rea}) is calculated as follows:

$$\Delta G_{act} = G_{FS} - G_{IS} \quad (4)$$

where G_{FS} is the free energy of the final state.

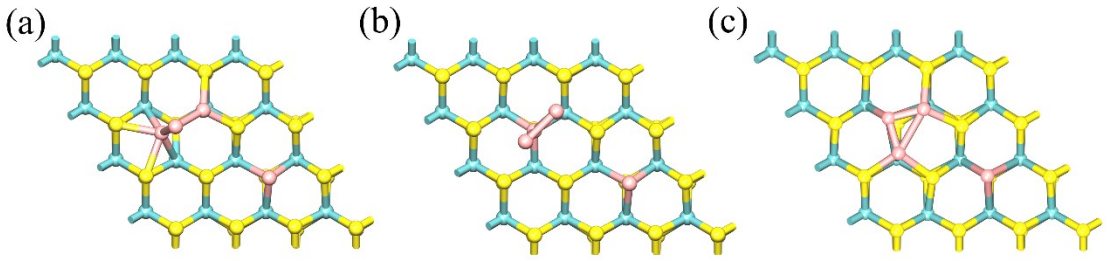

Fig. S1. Tuning of the Ru_3 site configuration in the synergistic Ru_1-Ru_3@MoS_2 catalyst. (a) Perpendicular placement of the Ru_3 cluster; (b) Inverted placement of the Ru_3 cluster; (c) Parallel placement of the Ru_3 cluster.

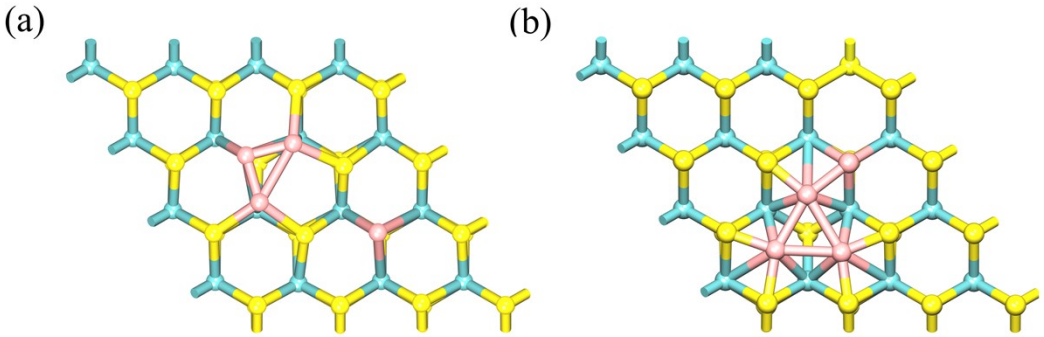

Fig. S2. The influence of different sulfur vacancy positions on the catalyst structure, (a) distant vacancy; (b) adjacent vacancy.

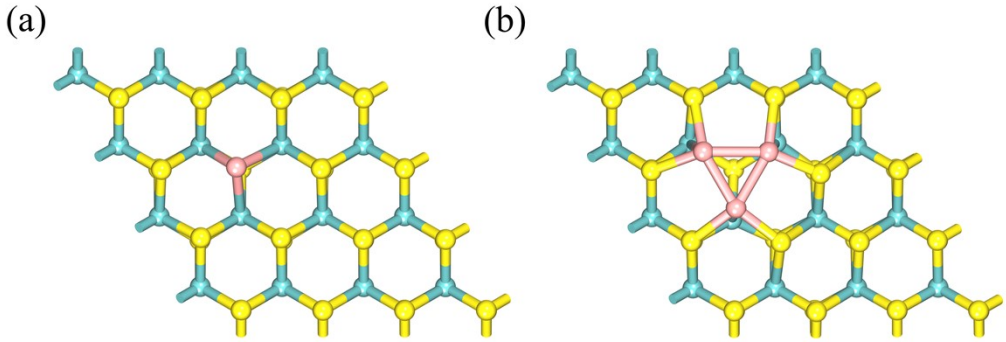

Fig. S3. The reference catalysts formed by loading Ru single atom or Ru_3 cluster alone. (a) Ru_1@MoS_2; (b) Ru_3@MoS_2.

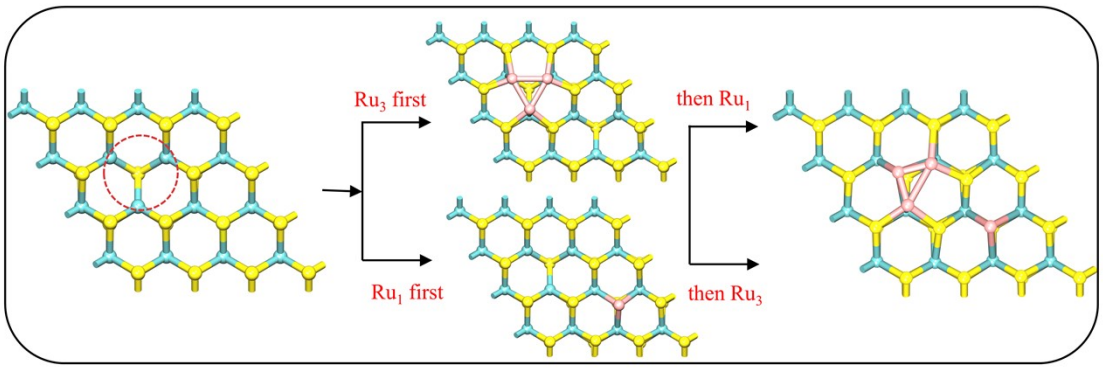

Fig. S4. Construction of the Ru_1-Ru_3@MoS_2 catalyst under different loading sequences.

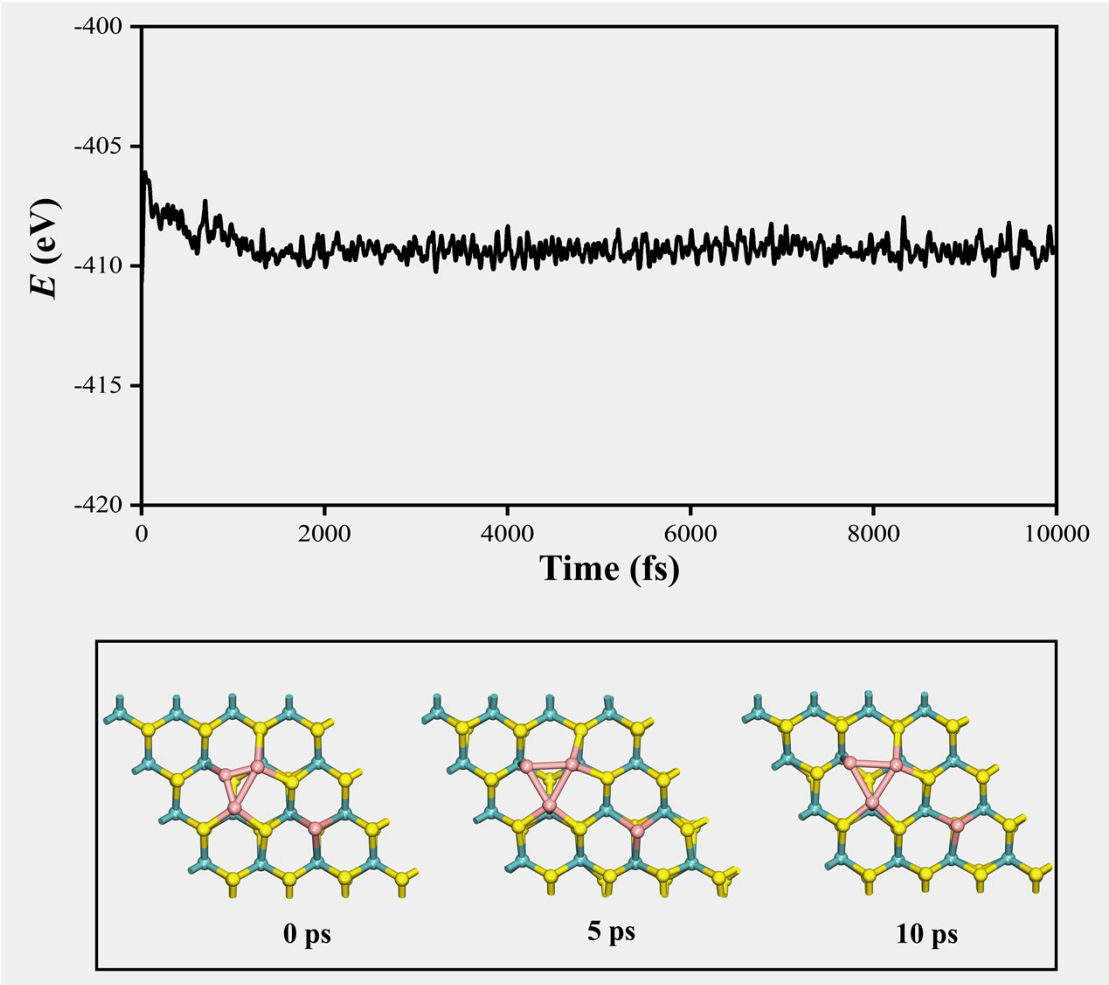

Fig. S5. Energy evolution trend and structural snapshots at different time points of the Ru_1-Ru_3@MoS_2 system in 0-10 ps neural network molecular dynamics simulations.

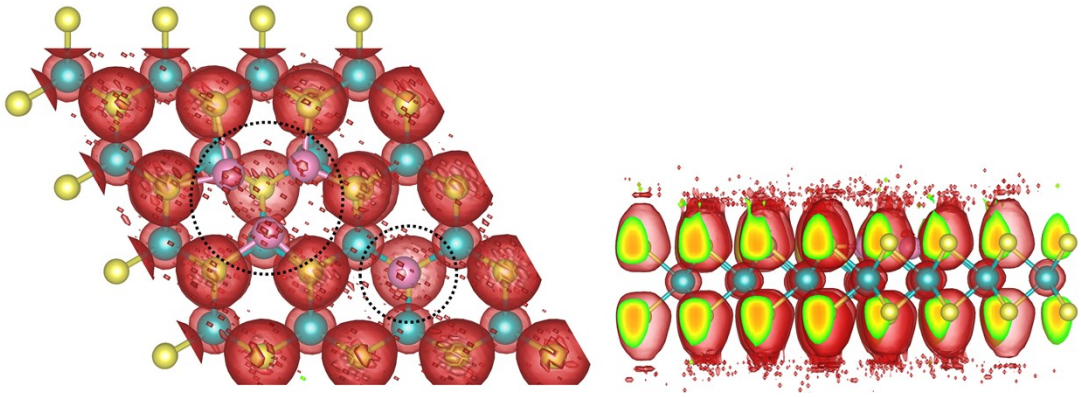

Fig.S6. The three dimensional distribution of electron localization function map. Red regions indicate electron density accumulation, the black dashed circle indicates the electron delocalization region of the Ru species.

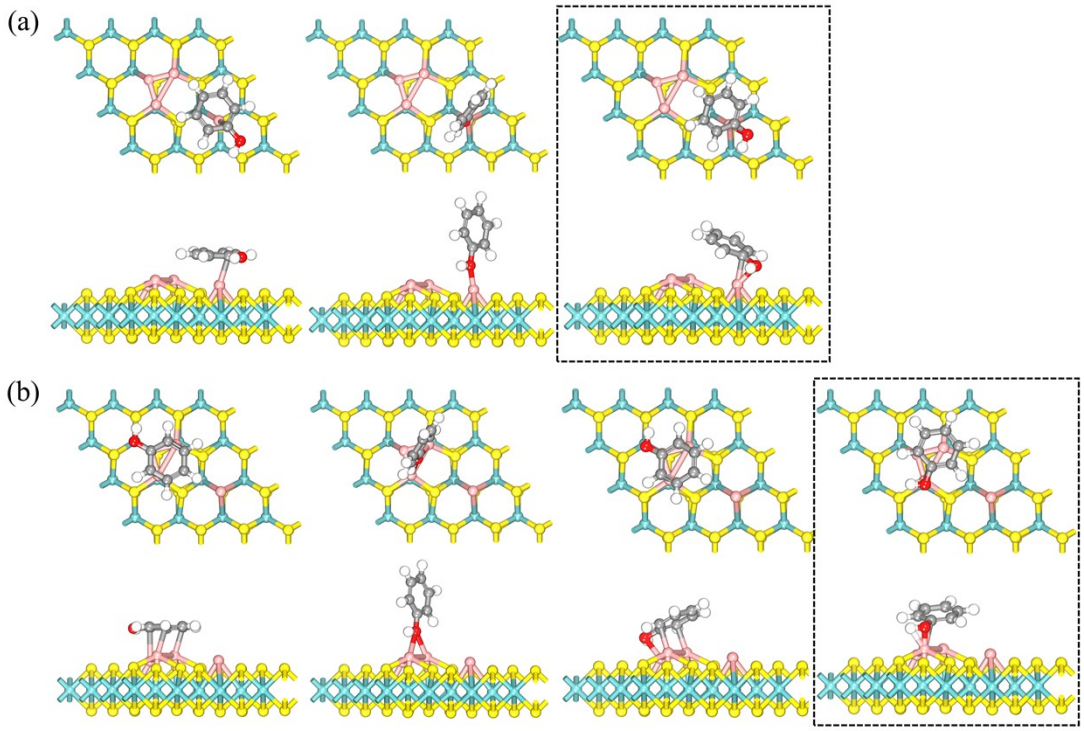

Fig. S7. Parallel, Vertical, and inclined adsorption configurations of phenol for (a) Ru_1-i-ad (b) Ru_3-i-ad (S, yellow; Mo, green; Ru, pink; C, gray; H, white).

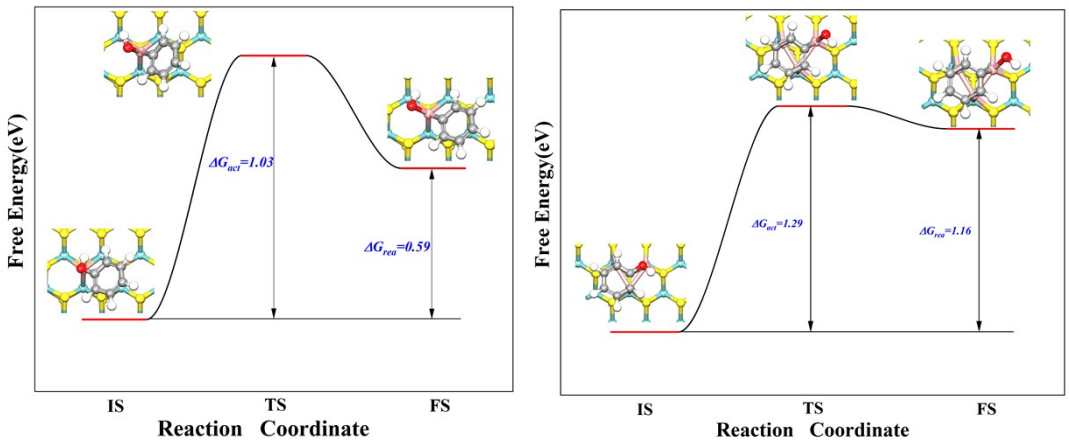

Fig. S8. Activation energy barriers of $Ru_1@MoS_2$ and $Ru_3@MoS_2$ for the C-O bond cleavage in the first elementary step.

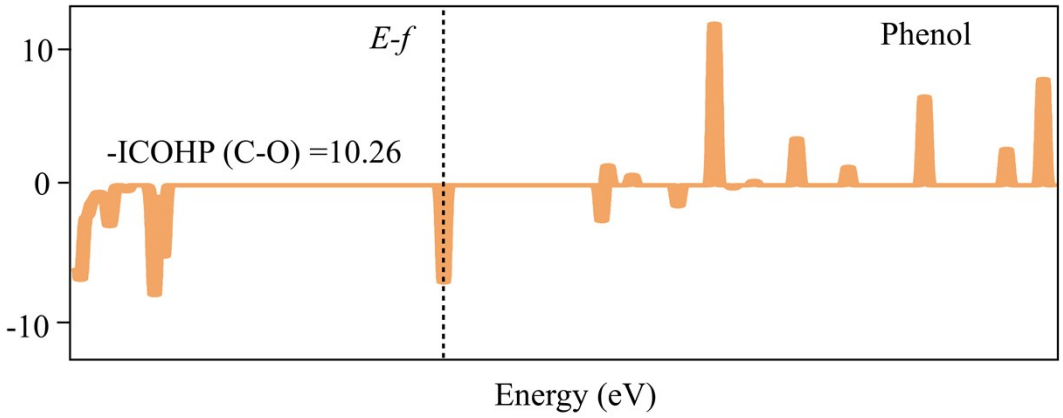

Fig. S9. Schematic of the COHP for the C-O bond in free gaseous phenol before adsorption.

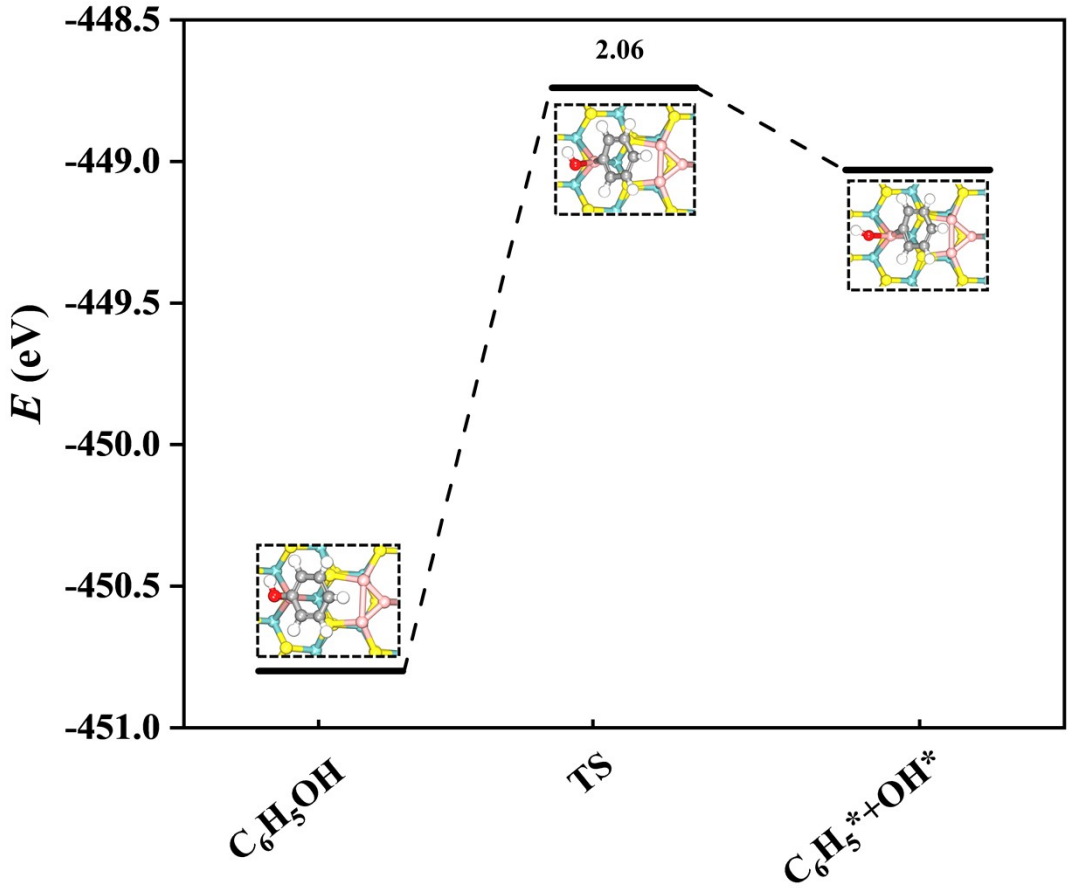

Fig. S10. Minimum energy pathway for the step $C_6H_5OH^* \rightarrow TS1 \rightarrow C_6H_5^* + OH^*$ in the main-text Fig. 3a, calculated with the catalyst substrate structurally constrained.

Table S1. Binding energies of catalysts corresponding to different Ru_3 placements in Ru_1-Ru_3@MoS_2.

reference catalysts	Perpendicular placement	Inverted placement	Parallel placement
E_b	-3.37	-3.38	-3.51

Table S2. Binding Energy of catalysts under different vacancy configurations.

reference catalysts	distant vacancy	adjacent vacancy
E_b	-3.51	-2.02

Table S3. Comparison of binding energies for the reference catalysts: Ru_1@MoS_2, Ru_3@MoS_2, and the synergistic Ru_1-Ru_3@MoS_2 system.

reference catalysts	Ru_1@MoS_2	Ru_3@MoS_2	Ru_1-Ru_3@MoS_2
E_b	-5.97	-2.87	-3.51

Table S4. Binding Energy of catalysts under different loading orders

Loading order	Ru_3 first, then Ru_1	Ru_1 first, then Ru_3
E_b	-1.05	-2.01

Table S5. Comparison of adsorption free energies (ΔG_{ads}) at the two sites of the catalyst.

Adsorption configuration	Parallel (eV)	Vertical (eV)	Inclined (eV)
Ru_1-i-ad	-0.53	-0.30	-0.82
Ru_3-i-ad	-2.10	-0.51	-1.97
			-2.27

Table S6. The free energies and the changes in Gibbs free energy of the initial state (IS), transition state (TS), and final state (FS) on the two active sites in the first elementary reaction, as well as those on their reference catalysts, were calculated and compared.

$C_6H_5OH^*$→TS1→$C_6H_5^*$+OH*	IS (eV)	TS (eV)	FS (eV)	ΔG_{act}	ΔG_{rea}
Ru_1-i-ad	-453.51	-452.84	-453.98	0.67	-0.47
Ru_3-i-ad	-448.02	-447.31	-447.91	0.71	0.11
Ru_1@MoS_2	-438.22	-437.19	-437.63	1.03	0.59
Ru_3@MoS_2	-454.24	-452.95	-453.08	1.29	1.16

Table S7. The C-O bond length of IS, TS and FS in the first elementary reaction.

$C_6H_5OH^*$→TS1→$C_6H_5^*$+OH*	IS_{LC-O} (Å)	TS_{LC-O} (Å)	FS_{LC-O} (Å)
Ru_1-i-ad	1.38	1.92	3.18
Ru_3-i-ad	1.38	1.90	2.34
Ru_1@MoS_2	1.40	2.03	2.61
Ru_3@MoS_2	1.37	2.16	2.38

Table S8. The free energies and the changes in Gibbs free energy of the initial state (IS),

transition state (TS), and final state (FS) on the two active sites in the second elementary reaction.

C_6H_5* + H*→TS2→C_6H_6*+OH*	IS (eV)	TS (eV)	FS (eV)	ΔG_{act}	ΔG_{rea}
Ru_1-i-ad	-458.03	-458.01	-459.90	0.02	-1.87
Ru_3-i-ad	-451.00	-450.51	-451.75	0.49	-0.75

Table S9. The C-H bond length of IS, TS and FS in the second elementary reaction.

C_6H_5* + H*→TS2→C_6H_6*+OH*	IS_{LC-H} (Å)	TS_{LC-H} (Å)	FS_{LC-H} (Å)
Ru_1-i-ad	2.55	2.10	0.96
Ru_3-i-ad	2.35	2.11	0.93

Table S10. The free energies and the changes in Gibbs free energy of the initial state (IS), transition state (TS), and final state (FS) on the two active sites in the third elementary reaction.

OH *+ H* → TS3 → H_2O*	IS (eV)	TS (eV)	FS (eV)	ΔG_{act}	ΔG_{rea}
Ru_1-i-ad	-460.78	-460.57	-461.52	0.21	-0.74
Ru_3-i-ad	-461.03	-460.74	-461.31	0.29	-0.28

Table S11. The O-H bond length of IS, TS and FS in the third elementary reaction.

OH *+ H* → TS3 → H_2O*	IS_{LO-H} (Å)	TS_{LO-H} (Å)	FS_{LO-H} (Å)
Ru_1-i-ad	2.34	1.56	1.11
Ru_3-i-ad	3.15	1.38	1.23

Table S12. Changes in magnetic moments across the elementary reaction steps.

Reaction	Spin Magnetic Moments(μ_B)
C_6H_5OH*	1.99
TS1	1.68
C_6H_5*+OH*	1.99
C_6H_5*+H*+OH*	0.99
TS2	1.19
C_6H_6*+ OH*	1.22
H*+OH*	0.00
TS3	3.95
H_2O*	1.99

Table S13. The distance between the Ru_1 single atom and the mass center of the Ru_3 cluster, denoted as $d_{SA\text{-}NC}$.

Reaction	$d_{SA\text{-}NC}$(Å)
C_6H_5OH*	4.94
TS1	4.30
C_6H_5*+OH*	4.14
C_6H_5* migration	4.52
C_6H_5*+H*+OH*	4.52
TS2	4.31
C_6H_6*+ OH*	4.84
C_6H_6	4.47
H*+OH*	4.27
TS3	4.94
H_2O*	4.84

Table S14. Energy change and C-O bond length variation during Ru_1-Ru_3@MoS_2 catalyzed C_6H_5OH* → TS1 → C_6H_5* reaction after substrate fixation.

	IS	TS	FS
E (eV)	-450.80	-448.74	-449.03
$d_{C\text{-}O}$ (Å)	1.38	1.93	2.54